

Experimental Fatigue Test for Pre-Qualification of Repair Mortars Applied to Historical Masonry

Original

Experimental Fatigue Test for Pre-Qualification of Repair Mortars Applied to Historical Masonry / Grazzini, A. - In: Advanced Engineering Testing / Aidy A.. - STAMPA. - London : IntechOpen, 2018. - ISBN 978-1-78984-243-2. - pp. 3-22 [10.5772/intechopen.79543]

Availability:

This version is available at: 11583/2715708 since: 2018-10-25T11:14:46Z

Publisher:

IntechOpen

Published

DOI:10.5772/intechopen.79543

Terms of use:

This article is made available under terms and conditions as specified in the corresponding bibliographic description in the repository

Publisher copyright

(Article begins on next page)

Experimental Fatigue Test for Pre-Qualification of Repair Mortars Applied to Historical Masonry

Alessandro Grazzini

Additional information is available at the end of the chapter

<http://dx.doi.org/10.5772/intechopen.79543>

Abstract

Restoration work on historical masonry buildings requires new repair materials capable of providing adequate durability over time. The interface between strengthening mortar and historical masonry can be the site of various stresses due to mechanical and thermo-hygrometric actions, also causing delamination actions. At the Non-Destructive Testing Laboratory of the Politecnico di Torino, an experimental methodology has been developed through static, freezing-thawing and cyclic tests on mixed mortar-bricks specimens. The aim of the laboratory tests was to select a durable and compatible repair mortar before the application. Fatigue tests simulated all main stresses that can be generated at the interface between repair mortar and original masonry, both mechanical and thermo-hygrometric aspects. The experimental results were interpreted by evaluating the variation of deformation parameters over time during the tests. From a range of four strengthening mortars, the experimental procedure was able to select the one with the greatest guarantees of durability and compatibility. A similar experimental procedure has also been developed to test the durability of dehumidified mortars suitable for the recovery of historical plasters subjected by rising damp effects. The same selected mortars have been used successfully at prestigious restoration sites, demonstrating their validity over time.

Keywords: strengthening mortars, historical masonry, durability, fatigue test, plaster detachment

1. Introduction

The architectural heritage requires significant recovery and strengthening work due to the high degradation to which it was abandoned. In particular, historical buildings present a lot of damage caused by mechanical stresses (seismic actions, structural failures, overloads) and

thermo-hygrometric stresses (freezing-thawing cycles, rising damp effects) that have reduced the masonry strength. Often the refurbishment projects require historical buildings to change their intended use with necessary structural retrofit. This study aims to focus on the use of structural mortars, useful both in the field of strengthening work (reinforced plasters, reinforcement of vaults, grout injections in the masonry textures) and in the restoration work (dehumidified plasters). The choice of new strengthening products must pay attention to their compatibility of the mechanical characteristics compared to those of the original masonry structures, often very heterogeneous [1]. The market offers many types of structural mortars, some with high mechanical performance, of which only short-term resistance values are declared, but nothing is known about their durability when applied to very heterogeneous masonry structures.

The historical masonries have very different mechanical characteristics due to the variegated building textures and the specific degradation's level. Therefore, a single structural mortar cannot have the mechanical and thermo-hygrometric characteristics compatible with all diverse historical masonries. Unfortunately, some restoration works, carried out by high-performance cement mortars, have failed registering detachments of the strengthening products from the masonry supports.

Recent earthquakes have shown the clear failure of restoration work performed with the use of concrete materials, the excessive stiffness of which has completely distorted the original characteristics of historical masonry buildings. **Figure 1** shows the ineffectiveness of the cementitious insertion materials inside historical walls of the St. Agostino church, collapsed during the last great Italian earthquake of Amatrice, just in correspondence with the previous stitching made by cement injections.

In many instances, the strengthening work, performed with the parameters of modern technologies, has modeled the buildings through static schemes that are not suitable for old structures. They can produce a notable difference in mechanical performances compared to historical masonry, which can generate dangerous stresses to the interfaces among the materials. On the contrary, it is necessary to prefer the use of mortars based on hydraulic lime with mechanical characteristics similar to those of historical masonries. In addition, each wall texture deserves an ad hoc experimentation in order to evaluate, among a range of products offered by the market, which structural mortar has the most compatible mechanical and thermo-hygrometric characteristics, and therefore ensure greater durability of the intervention. Therefore, only the coupling between two materials with the same characteristics and similar elastic modulus will guarantee the mutual collaboration between the two materials, avoiding detachments.

At the Non-Destructive Testing Laboratory of the Politecnico di Torino, an experimental procedure was set up to select the new structural mortars and test their durability when applied to a specific historical masonry texture. The goal of this research is to show the fundamental importance of preliminary tests to identify the most compatible product for each specific restoration work. The procedure can be useful for the designer who needs to choose the best mortar, which guarantees durability over time when applied to a specific masonry structure. The tests are intended to simulate stresses under different mechanical and thermo-hygrometric actions that may occur in the useful life of the restored building. The tests are both static and cyclical, and start from single specimens to characterize the single material up to mixed



Figure 1. Collapse of the St. Agostino church in Amatrice after the Central Italy earthquake 2016 (image courtesy of the Curia of Rieti).

mortar-brick specimens that have the function of simulating the real stresses that over time can undermine the structural binomial.

A first part of the tests concerns the validation of structural mortars for strengthening work, which must be carried out at the restoration site of the Royal Palace of Venaria. The second part concerns a similar methodology to test the adhesion of dehumidified plasters applied to historical masonry walls of the Sacro Monti di Varallo heritage site. Two important restoration sites have demonstrated over time the validity of the use of the repair mortars selected during the experimental procedure that will be described.

2. Validation of structural mortar for strengthening work at the Royal Palace of Venaria

The Royal Palace of Venaria, a UNESCO site near Turin, is one of the most famous monuments in Italy. His recovery project was among the most important in Europe (**Figure 2**). The restoration site has also been the place of experimentation with new techniques and materials for structural reinforcement methods. Within the restoration site, a research agreement was set up in collaboration with the Non-Destructive Testing Laboratory of the Politecnico di Torino, with the aim of validating the durability of the repair mortars used in subsequent strengthening and restoration work [2].



Figure 2. The Royal Palace of Venaria.

2.1. Experimental materials and setup

To determine the main mechanical characteristics of the individual materials, that is, the compressive strength and the elastic modulus, six specimens $40 \times 40 \times 160$ mm were manufactured for each single material. Four different types of mortars were tested (codified as “A,” “B,” “C,” “D”), suitable for the following restoration techniques: reinforcement by structural plaster (A; C), joint closing (A; D), jacketing of masonry walls or reinforcement of vaults (D), consolidation by grout injection (B). In addition to these, six more specimens $40 \times 40 \times 160$ mm made from historic bricks of the Royal Palace of Venaria were tested (Figure 3). Each mortar test piece was labeled with “XM” where “X” stands for the code of the relative mortar (A–D); the brick test piece was labeled with “LT.”

The next step of this experimental procedure was the manufacturing of particular mixed brick-mortar specimens measuring $223 \times 57 \times 83$ mm (Figure 4). The mixed specimens were made from historical cut on which a 30 mm thick layer of strengthening mortar was applied. The brick surface was treated by means of a drill to facilitate the mortar’s adhesion. The treatments simulate roughness and irregularity of the masonry surface that in the real executive

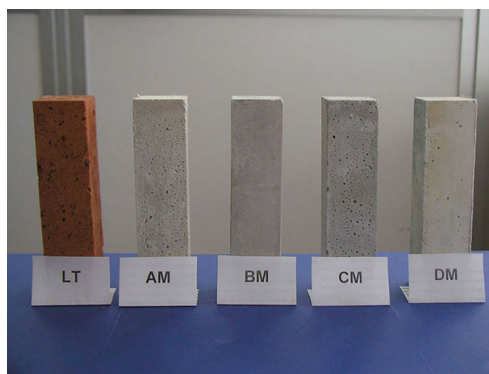


Figure 3. Single specimens.

phases can improve the adhesion of strengthening plaster, or the irregular inside masonry texture that can improve the adhesion of a fluid injection mortar.

Each mixed test piece was labeled with “XL” where “X” stands for the code of the relative mortar (A–D).

Altogether eight mixed pieces were manufactured for each “XL” series: two for preliminary static tests, three for freezing-thawing tests and three for cyclic loading tests. The vertical and horizontal displacements were recorded respectively by means of a couple of vertical transducers and a horizontal transducer (**Figure 4**). The horizontal transducer served to measure the displacements due to bulging. The mixed specimens were instrumented also with a pair of electrical strain gauges on the opposing vertical faces measured transverse strains. In this manner, it is possible to measure the axial deformations (in vertical, horizontal and transverse directions), whose algebraic sum yields the volumetric deformation.

Cyclic and static compressive tests were carried out by means of a 250 kN model 810 MTS. Freezing-thawing cycles were performed through a laboratory oven and a refrigerator cell.

2.2. Mechanical and thermo-hygro-metric characteristics of single materials

The results of static tests on single materials are shown in **Table 1**. Because of a technical hitch in the number of manufactured specimens, only for mortar B and D, the evolution of

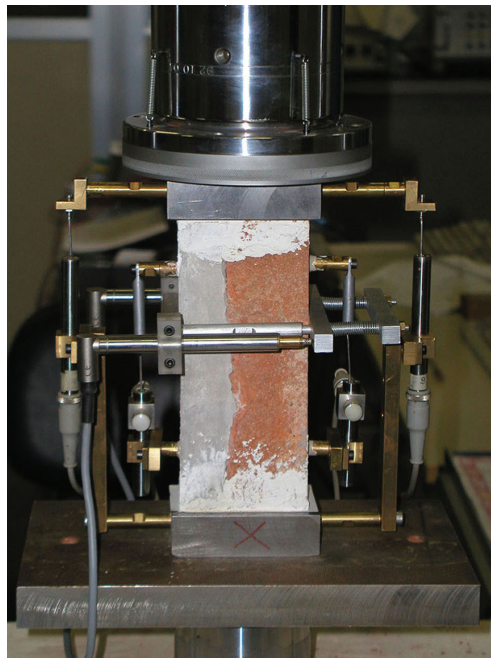


Figure 4. Mixed brick-mortar test pieces.

mechanical characteristics in the time due to the maturation effects has been analyzed, verifying that the changes in mechanical behavior are remarkable (**Tables 2 and 3**).

The analysis of the effects of the adverse environmental conditions (seasonal temperature ranges) was carried out by freezing-thawing tests on mortars B and D specimens (**Table 4**). None of the test piece B remained intact to reach the minimum threshold of 25 cycles. On the contrary, mortar D after 25 cycles showed a significant increase in resistance (+34.27%). After 50 cycles, there is a decrease in compressive strength again, bringing the average values close to the virgin reference (−3.12%). The reason for these substantial changes in mechanical properties may be due to thermal changes in the chemical base of the product [3]. However, these changes are very important and must be taken into account in the durability of the strengthening materials over time. These experimental results demonstrate the need to perform fatigue tests on repair materials before their use. A strong change in the mechanical characteristics of the strengthening materials can make it over time incompatible with the mechanical performance of the historical masonries on which it has been applied, favoring its detachment.

2.3. Experimental results of mixed test pieces

Table 5 shows the main mechanical characteristics of mixed test specimens. The mechanical performances after 28 freezing-thawing cycles are shown in **Table 6**, observing a great increase of strength.

The main phase of this validation procedure was the cyclic tests. The high value selected for cyclic load (70% of static load) was designed to make the test severe enough despite the short duration in the time (1,00,000 cycles—1.3 Hz), and to highlight the potential of several indicators monitored over time. The evolution of the volumetric deformation of mixed pieces was analyzed. Its propensity to negative values (increase in volume) can reflect a lesser degree of collaboration between the two materials, or even their detachment at the interface.

The test setup was performed through four steps:

- initial 70% loading-unloading test (3 cycles);
- 70% cyclic test (1,00,000 cycles);
- final 70% loading-unloading test (1 cycle);
- postcyclic compression test to failure.

| Materials | E (N/mm ²) | ν | σ (N/mm ²) | $\Delta\% \sigma$ |
|-----------------------|------------------------|-------|-------------------------------|-------------------|
| Mortar A | 6208 | 0.12 | 8.27 | −7.50 |
| Mortar B | 7534 | 0.19 | 10.91 | +111.55 |
| Mortar C | 12,678 | 0.23 | 10.34 | +146.39 |
| Mortar D | 12,274 | 0.32 | 24.95 | +57.47 |
| Historical brick (LT) | 4099 | 0.08 | 8.09 | — |

E = elastic modulus, ν = Poisson's coefficient, σ = failure stress, $\Delta\sigma$ = variation of σ .

Table 1. Elastic modulus and compression results of individual materials (40 × 40 × 160 mm).

| Test piece | Days | σ (N/mm ²) | $\Delta\% \sigma$ (28 days) | E (N/mm ²) | $\Delta\% E$ (28 days) |
|----------------|------------|-------------------------------|-----------------------------|------------------------|------------------------|
| BM 4.1 | 28 | 12.38 | | 7262 | |
| BM 7.3 | 28 | 12.54 | | 6960 | |
| BM 9.3 | 28 | 11.32 | | 7944 | |
| Average | 28 | 12.08 | — | 7389 | — |
| BM 3.3 | 90 | 19.74 | | 10,676 | |
| BM 1.3 | 90 | 19.59 | | 10,089 | |
| BM 10.2 | 90 | 20.37 | | 11,290 | |
| Average | 90 | 19.90 | +64.71 | 10,685 | +44.62 |
| BM 2.2 | 150 | 17.24 | | 8347 | |
| BM 6.1 | 150 | 20.02 | | 7923 | |
| BM 6.2 | 150 | 20.22 | | 9046 | |
| Average | 150 | 19.16 | +58.61 | 8439 | +14.21 |
| BM 2.3 | 210 | 17.47 | | 12,000 | |
| BM 8.1 | 210 | 17.94 | | 10,223 | |
| BM 3.1 | 210 | 19.02 | | 9680 | |
| Average | 210 | 18.14 | +50.16 | 10,634 | +43.92 |

σ = failure stress, E = elastic modulus, $\Delta\sigma$ = variation of σ , ΔE = variation of E.

Table 2. Mechanical characteristics during maturation of strengthening mortar B.

In the curve of a cyclic fatigue test (**Figure 5**), it is possible to identify three distinct stages:

- Stage I: Deformations are seen to increase rapidly (accounting for approximately 10% of the service life of test piece);
- Stage II: Deformations increase gradually at a virtually constant stress (10–80% of test piece life);
- Stage III: Deformations increase rapidly until failure [2].

Fatigue life of a material subjected to cyclic loading tests is linked to the evolution of the deformations during stage II [4–7]. By analogy with the method suggested for concrete [8], the evolution of vertical deformations over time was recorded for evaluating fatigue strength of material. The goal is to ascertain whether fatigue life of the mixed brick-mortar system also depends on the rate of increase of vertical deformations during stage II (termed secondary creep rate). **Figures 6–9** shows that the broken test pieces (before 1,00,000 cycles, as shown in **Table 7**) displayed a steeper slant in the stage II section of the curve, followed, at ca 80–90% of test piece life, by a sudden increase at stage III (failure). Conversely, the diagrams of the mixed specimens that passed 1,00,000 cycles mark displayed a lesser slant, reflecting an effective behavior still far from failure. From these results of cyclic tests, through linear interpolation between 20 and 80% of secondary creep values (**Figure 10**), derivatives $\partial \epsilon_v / \partial n$ (i.e., the

| Test piece | Days | σ (N/mm ²) | $\Delta\% \sigma$ (28 days) | E (N/mm ²) | $\Delta\% E$ (28 days) |
|----------------|------------|-------------------------------|-----------------------------|------------------------|------------------------|
| DM 4.3 | 28 | 20.08 | | 9886 | |
| DM 6.2 | 28 | 20.97 | | 10,957 | |
| DM 7.3 | 28 | 20.87 | | 11,231 | |
| Average | 28 | 20.64 | — | 10,691 | — |
| DM 9.3 | 90 | 28.33 | | 12,455 | |
| DM 5.3 | 90 | 28.32 | | 12,907 | |
| DM 9.1 | 90 | 28.09 | | 11,947 | |
| Average | 90 | 28.25 | +36.87 | 12,436 | +16.32 |
| DM 1.1 | 150 | 28.99 | | 12,849 | |
| DM 10.2 | 150 | 28.46 | | 13,152 | |
| DM 6.2 | 150 | 28.10 | | 10,448 | |
| Average | 150 | 28.52 | +38.18 | 12,150 | +13.64 |
| DM 10.1 | 210 | 28.91 | | 12,406 | |
| DM 6.3 | 210 | 29.16 | | 14,821 | |
| DM 2.2 | 210 | 29.66 | | 16,177 | |
| Average | 210 | 29.24 | +41.70 | 14,468 | +35.32 |

σ = failure stress, E = elastic modulus, $\Delta\sigma$ = variation of σ , ΔE = variation of E.

Table 3. Mechanical characteristics during maturation of strengthening mortar D.

| Test Piece | Cycles | σ_i (N/mm ²) | σ_f (N/mm ²) | $\Delta\sigma\%$ (0-cycles) | E_i (N/mm ²) | E_f (N/mm ²) | $\Delta E\%$ (0-cycles) |
|----------------|-----------|---------------------------------|---------------------------------|--------------------------------|----------------------------|----------------------------|-------------------------|
| DM 1.2 | 25 | 20.64 | 29.66 | +43.70 | 13,557 | 11,119 | -17.98 |
| DM 8.2 | 25 | 20.64 | 25.59 | +23.98 | 13,201 | 10,376 | -21.40 |
| DM 5.2 | 25 | 20.64 | 27.88 | +35.08 | 11,066 | 11,257 | +1.73 |
| DM 3.2 | 25 | 20.64 | — | — | 11,841 | 13,386 | +13.05 |
| DM 4.2 | 25 | 20.64 | — | — | 8826 | 12,167 | +37.85 |
| DM 7.1 | 25 | 20.64 | — | — | 9003 | 7869 | -12.59 |
| Average | 25 | 20.64 | 27.71 | +34.27 | 11,249 | 11,029 | -1.95 |
| DM 3.2 | 50 | 20.64 | 24.08 | +16.67 | 11,841 | 12,930 | +9.20 |
| DM 4.2 | 50 | 20.64 | 17.37 | -15.84 | 8826 | 10,453 | +18.43 |
| DM 7.1 | 50 | 20.64 | 18.53 | -10.22 | 9003 | 8418 | -6.50 |
| Average | 50 | 20.64 | 19.99 | -3.12 | 11,249 | 10,600 | -5.77 |

σ_i = failure stress, σ_f = freezing-thawing cycles, $\Delta\sigma\%$ = variation of σ after freezing-thawing test, $\Delta E\%$ = variation of E after freezing-thawing test.

Table 4. Static tests after freezing-thawing cycles on strengthening mortar D.

| Series | Test piece | P _{max} (kN) | σ _{max} (N/mm ²) | σ _{average} (N/mm ²) | E (N/mm ²) |
|--------|------------|-----------------------|---------------------------------------|---|------------------------|
| AL | AL02 | 102.75 | 19.30 | 15.40 | 11,988 |
| | AL04 | 59.76 | 11.49 | | 14,157 |
| BL | BL01 | 108.51 | 22.17 | 16.89 | 16,940 |
| | BL02 | 52.30 | 11.60 | | 4400 |
| CL | CL01 | 40.78 | 9.71 | 12.58 | 6597 |
| | CL02 | 76.98 | 15.46 | | 12,478 |
| DL | DL01 | 58.50 | 12.10 | 12.04 | 6191 |
| | DL02 | 60.45 | 11.98 | | 8106 |

P_{max} = failure load, σ_{max} = failure stress, E = elastic modulus.

Table 5. Results of preliminary static tests on mixed test pieces.

| Series | Test piece | Condition | P _{max} (kN) | σ _{max} (N/mm ²) | σ _{average} (N/mm ²) | Δσ% | E (N/mm ²) |
|--------|------------|-----------|-----------------------|---------------------------------------|---|--------|------------------------|
| AL | AL03 | Cracked | 95.54 | 19.78 | 15.88 | +3.15 | 10,050 |
| | AL06 | Detached | 81.00 | 15.83 | | | 8151 |
| | AL08 | Detached | 59.30 | 12.03 | | | 6701 |
| BL | BL07 | Cracked | 76.30 | 14.23 | 13.88 | -17.81 | 6250 |
| | BL10 | Cracked | 66.50 | 13.52 | | | 6582 |
| CL | CL06 | Whole | 104.50 | 19.92 | 15.52 | +18.25 | 10,604 |
| | CL08 | Whole | 54.62 | 11.13 | | | 7191 |
| DL | DL08 | Whole | 107.40 | 21.52 | 22.87 | +89.93 | 35,358 |
| | DL07 | Whole | 129.30 | 24.22 | | | 16,249 |

P_{max} = failure load, σ_{max} = failure stress, Δσ% = variation of σ after freezing-thawing tests, E = elastic modulus.

Table 6. Results of static tests after freezing-thawing cycles.

variations in the deformation versus time curve during stage II) were calculated. Through a linear regression on logarithmic scale, it is possible to plot the data in a diagram in order to obtain an analytical relationship (1) between secondary creep variations, $\partial\epsilon_v/\partial n$, and the number of cycles (N) to fatigue failure:

$$N = 1839.92 \cdot \left(\frac{\partial\epsilon_v}{\partial n} \right)^{-0.7284} \quad (1)$$

A valid correlation was established between secondary creep rate ($\partial\epsilon_v/\partial n$) during stage II and fatigue life (number of cycles to failure, N). By performing a certain number of cycles on the material until deformations increase at a constant rate, it is possible to predict fatigue life with a good degree of approximation [9–11].

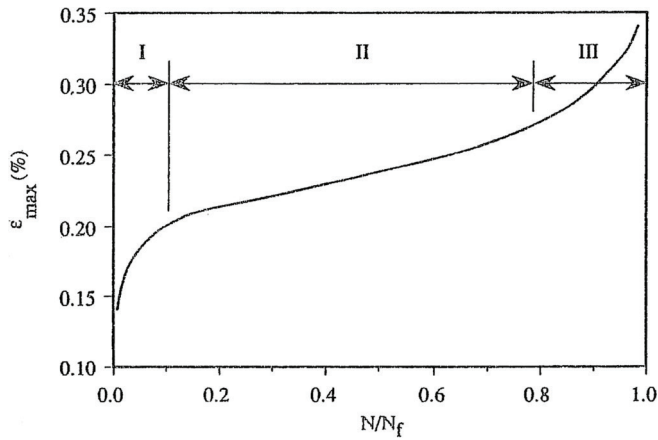


Figure 5. Monoaxial cycles compression test σ - ϵ curve.

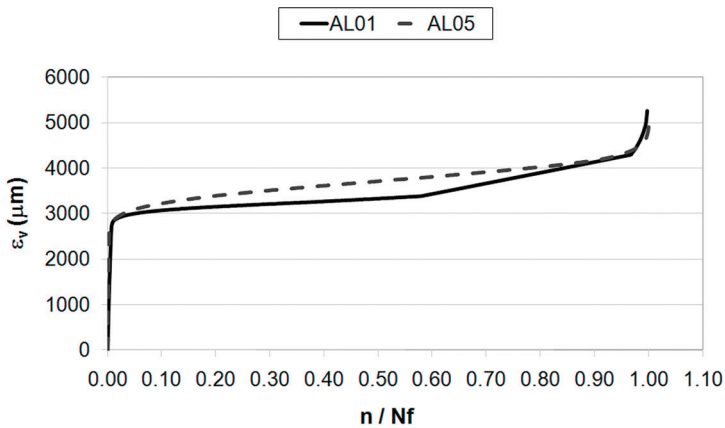


Figure 6. AL series cyclic tests: max vertical deformation.

In some samples, the theoretical value of cycles to failure N_{the} was found to be lower than that obtained from laboratory tests (Table 7). After the final value of cyclic test, the relationship (Eq. (1)) was useful to predict the failure on the detachment surface between brick and repair mortar. The measure of the volumetric deformations is in agreement with the theoretical value obtained from Eq. (1): the time when the volumetric deformations shifted to negative sign (propensity to bulge due to poor vertical collaboration or detachment at the interface between the two materials) was the failure time of the mixed brick-mortar specimen. The methodology and the numerical analysis proved very sensitive to the initial signs of weakening in the brick-mortar system, indicating clearly the onset of a crisis due to fatigue. Figures 11–14 illustrate the static tests performed on mixed test pieces.

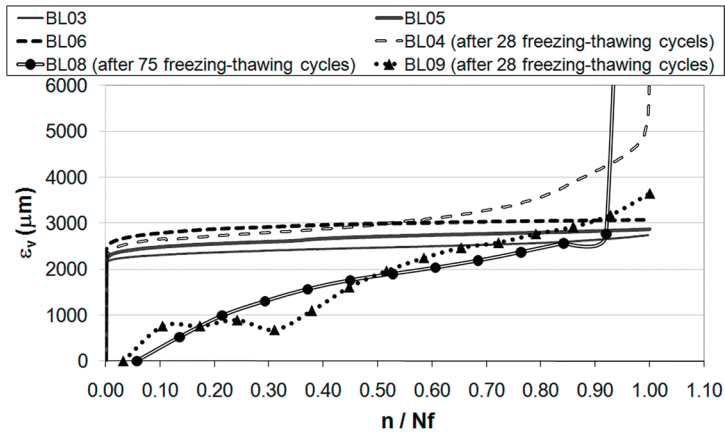


Figure 7. BL series cyclic tests: max vertical deformation.

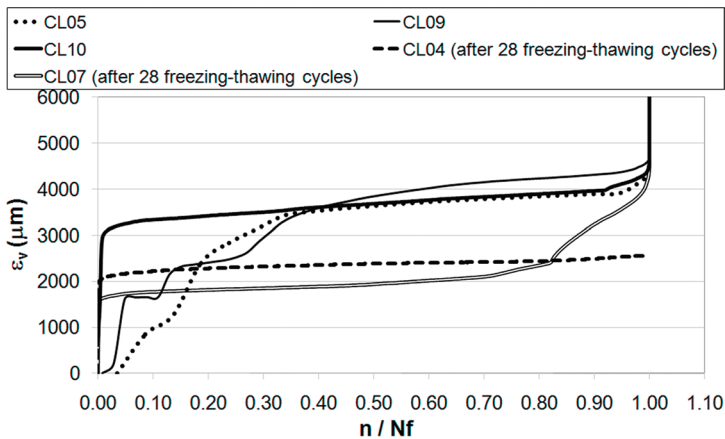


Figure 8. CL series cyclic tests: max vertical deformation.

The values obtained for a majority of the series remained within the average of the two preliminary tests, save for the series DL (Figure 14), which displayed a considerable increase in strength. In most cases, static curves after freezing-thawing revealed a more brittle behavior. Test pieces of BL and DL series that passed 1,00,000 cycles mark were tested to failure: the DL series displayed a noticeable increase of their mechanical properties. Some CL and DL test pieces were subjected both to freezing-thawing test and to cyclic loading: CL maintained a static behavior similar to the weakest preliminary test result; instead in the DL series, an appreciable increase of strength was mated to a lesser degree of brittleness compared to the test pieces subjected to cyclic loading only.

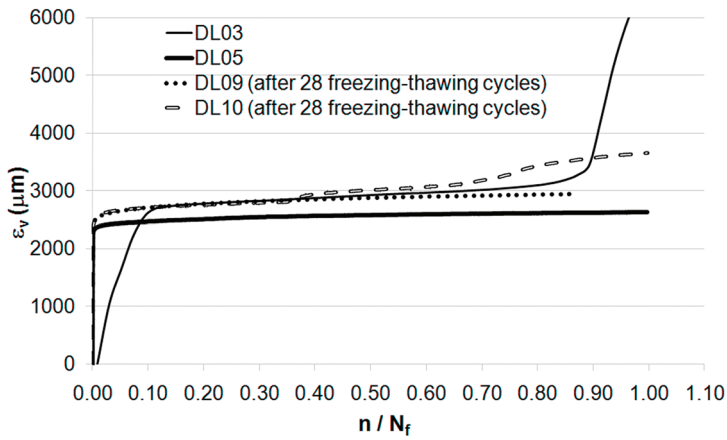


Figure 9. DL series cyclic tests: max vertical deformation.

| Test piece | n | $\partial \epsilon_v / \partial n$ | LogN | Log($\partial \epsilon_v / \partial n$) | N_{the} |
|------------|----------|------------------------------------|-------|---|-----------|
| AL01 | 22,380 | 0.0270 | 4.350 | -1.569 | 25,583 |
| AL05 | 53,465 | 0.0198 | 4.728 | -1.703 | 32,029 |
| BL03 | 1,00,000 | 0.0047 | 5.000 | -2.323 | 90,605 |
| BL05 | 1,00,000 | 0.0040 | 5.000 | -2.398 | 102,716 |
| BL06 | 1,00,000 | 0.0024 | 5.000 | -2.612 | 147,056 |
| CL05 | 461 | 5.1818 | 2.664 | 0.714 | 555 |
| CL09 | 1223 | 2.5110 | 3.087 | 0.400 | 941 |
| CL10 | 15,835 | 0.0501 | 4.200 | -1.300 | 16,294 |
| DL03 | 1149 | 0.4704 | 3.060 | -0.328 | 3187 |
| DL05 | 1,00,000 | 0.0015 | 5.000 | -2.813 | 206,028 |
| DL06 | 1,00,000 | 0.0070 | 5.000 | -2.155 | 68,328 |
| BL04 | 40,993 | 0.0340 | 4.613 | -1.469 | 21,612 |
| BL09 | 360 | 9.4729 | 2.556 | 0.976 | 358 |
| CL04 | 1,00,000 | 0.0035 | 5.000 | -2.454 | 112,832 |
| CL07 | 46,622 | 0.0192 | 4.669 | -1.717 | 32,795 |
| DL09 | 1,00,000 | 0.0025 | 5.000 | -2.594 | 142,671 |
| DL10 | 1,00,000 | 0.0113 | 5.000 | -1.947 | 48,171 |

Table 7. Analysis of the data.

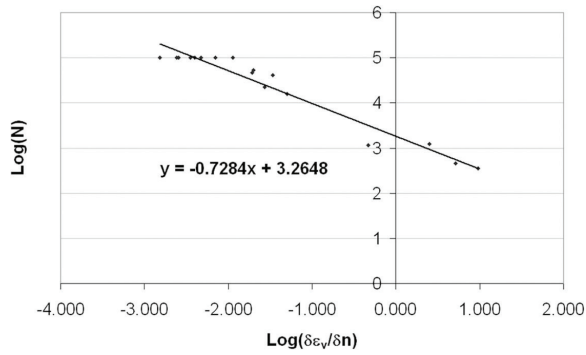


Figure 10. Fatigue life of mixed test pieces $\delta\varepsilon_v/\delta n$ chart.

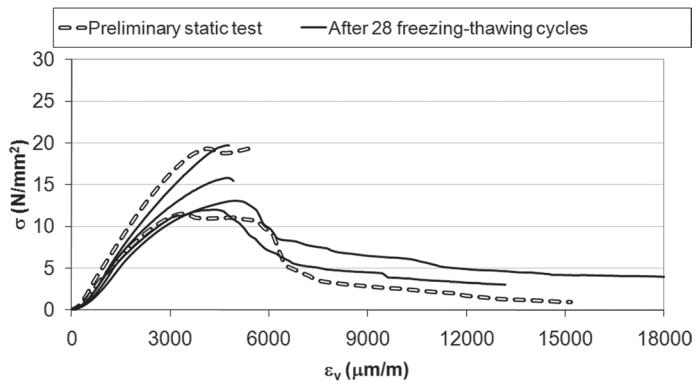


Figure 11. AL series static tests.

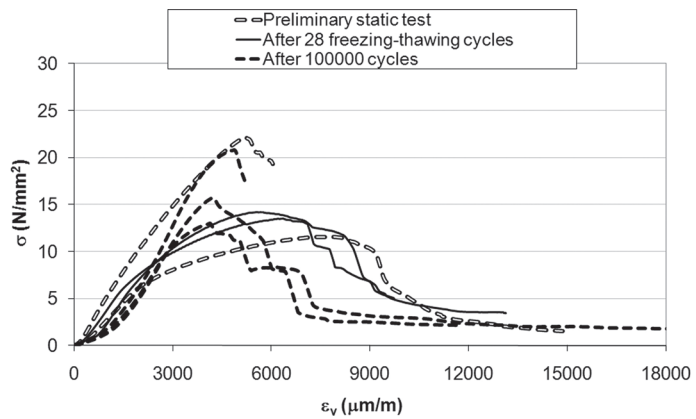


Figure 12. BL series static tests.

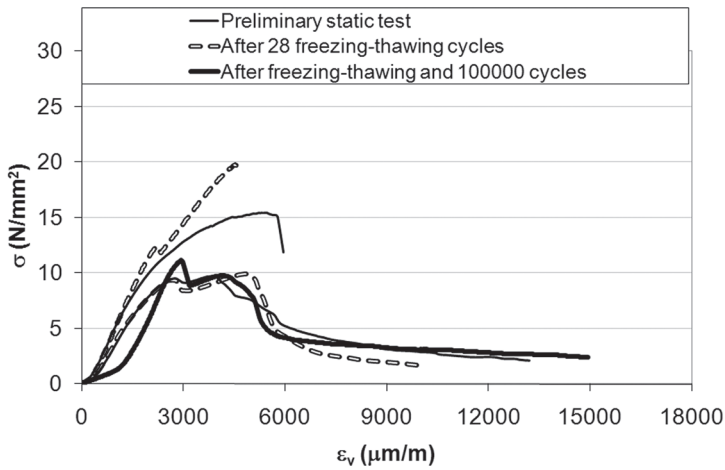


Figure 13. CL series static tests.

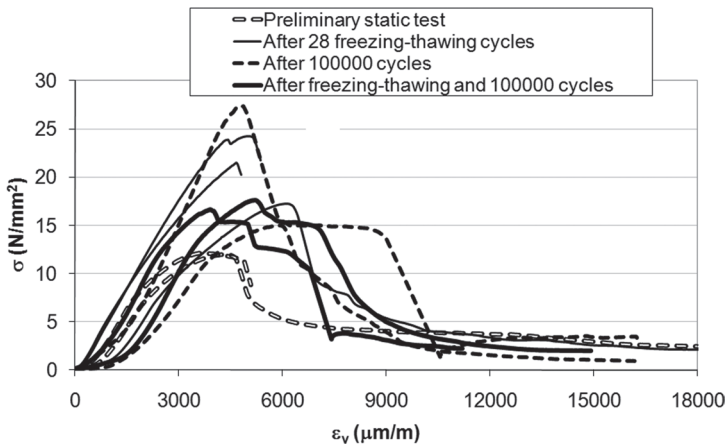


Figure 14. DL series static tests.

2.4. Selection of optimal mortar

From the results of this experimental procedure, mortar D was chosen for the best compatible characteristics because, compared with the other mortars, during fatigue and freezing-thawing tests, these strengthening materials showed the greatest number of cycles without excessive variations of mechanical characteristics.

The choice of mortar D also was confirmed by the good results of preliminary tests, performed in situ. From six double flat jack tests, a value of failure tension σ average was found equal to 1.91 N/mm² in accord with that (1.61 N/mm²) obtained by laboratory tests on the big masonry walls, manufactured by original bricks and stones extracted in situ. The positive confirmation



Figure 15. Application of mortar D as the reinforced plaster to Venaria's masonries.

came from the real application of mortar D as reinforced plaster retrofitting of some walls of the Royal Palace of Venaria (**Figure 15**). After 10 years, this plaster does not present any pathology of incompatibility.

3. Experimental procedure for selecting a durable dehumidified mortar

Often masonry walls of historical buildings are subject to rising damp effects due to capillary or rain infiltrations. In the time, their cyclic action produces decay and delamination of historical plasters. The restoration market offers a great number of dehumidified repair mortars to use as new transpiring plasters. Nevertheless, their mechanical and thermo-hygrometric characteristics have not been compared carefully with those of the historical masonry supports, often producing the failure of restoration work. Preventing this phenomenon is the main way of increasing the durability of repair work [12].

An innovative laboratory procedure, developed at the Non-Destructive Testing Laboratory of the Politecnico di Torino, is described for test mechanical adhesion of new repair mortars. Compression static tests were carried out on composite specimen stone block-repair mortar, which specific geometry can test the de-bonding process of mortar in adherence with a stone masonry structure. The methodology is being used at Sacro Monte di Varallo Special Natural Reserve. Situated at the top of the hill above the town of Varallo in Piedmont (Italy), Sacro Monte is an artistic-religious complex consisting of 45 chapels, which contain with frescoes and sculptures that tell the story of the life of Christ (**Figure 16**).

The main problem of historical plasters' preservation is linked to the rain infiltrations and to the freezing-thawing cycles that compromise their adhesion to stone masonries. Through compression static tests on stone-mortar composite specimens, it was possible to prequalify the dehumidified mortar with greater durability guarantees. Sometimes the long-term detachment determined the failure of the restoration work. The test validates the mechanical



Figure 16. Decay of historical plasters because of the rain infiltrations (Sacro Monte of Varallo).

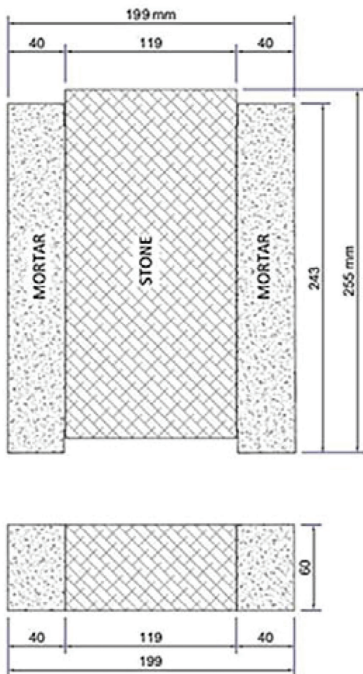


Figure 17. Geometry of composite specimen and test setup.

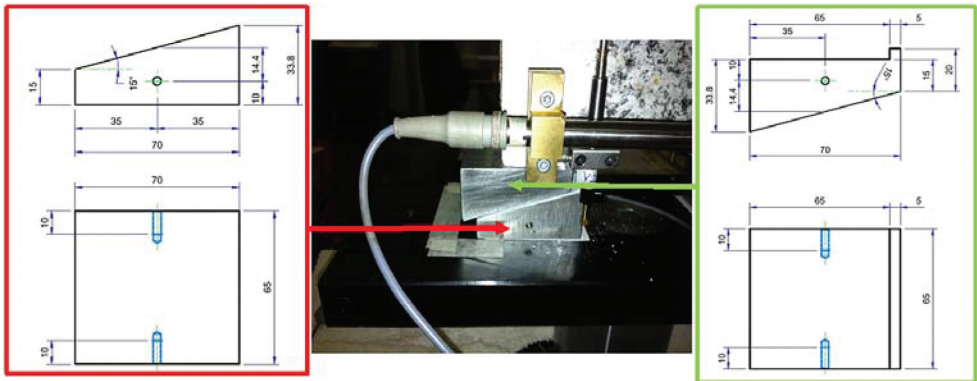


Figure 18. The wedges' geometry and test setup.

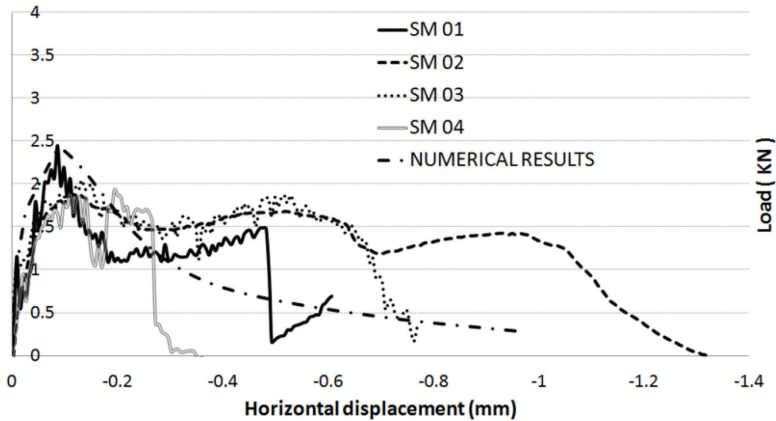


Figure 19. Load-horizontal displacement curves of static tests.

compatibility between the repair mortars and historical masonries stone, as a guarantee also for durability over time against atmospheric agents.

3.1. Preparation of the laboratory test

For carrying out tests, a particular geometry of the composite specimen has been proposed. Four mixed specimens were made, applying a 40 mm mortar layer to both shorter faces of the stone brick suitably cut with the dimensions shown in **Figure 17**. The mechanical characteristics of the repair mortar and the stone brick were chosen equivalent to those of the stone masonry at the Sacro Monte di Varallo. The experimental test can carry out also by masonry brick, if the historical walls were made by bricks. The hydraulic lime mortar was a pre-blended transpiring product, for dehumidifying repair work on historical masonry

damaged by dampness. For this mortar, the Young's modulus was 4379 MPa, and the compressive strength was 33.8 MPa.

The surface of the stone block has been treated specifically by means of a drill to facilitate the mortar's adhesion. This treatment aimed to simulate the real discontinuities on the wall surface that favor the adhesion of the plaster. The application of the dehumidified mortar took place leaving specific and surface symmetrical discontinuities at the top and bottom of the specimen, as shown in **Figure 17**. These notches favored the trigger and propagation of multiple cracks, in order to test the adhesion of two linked materials. An inductive horizontal displacement transducer was applied at the bottom of the specimen for the bulging displacements. The vertical displacements were recorded by the piston's translation of the 250 kN servo controlled test machine. The composite specimens were tested by monotonous compression load by horizontal controlled opening (0.0001 mm/s). Static tests have been performed after 28 days of maturation. The composite specimen rested, through the side layers mortar, on a double system of steel wedges (**Figure 18**). The wedges were coupled by a 1 mm thick Teflon layer for reducing the horizontal friction during the plaster's expansion. The "SM" (Stone brick-Mortar) label has been associated with each specimen with its sequence number.

3.2. Composite stone-repair mortar specimens

The results of compressive static tests are shown in **Figure 19**. A numerical simulation based on the cohesive crack model was used to follow the experimental data, in order to describe the evolutionary phenomenon of de-bonding as a function of a small number of parameters [13–15]. The composite specimen stone-mortar displayed four stress singularity points: two notch tips at the specimen's top, and two at the specimen's bottom. These points were the weakest planes involved in the singular stress fields. Because of the wedges, the cracks that start from the bottom of the specimen showed greater velocity than the cracks that start from the top of the specimen. To exception of SM 04, the other composite specimens were displayed a ductile behavior keeping a residual load and displacement after the peak load. That is a fundamental requirement for a durable service life of repair plasters subjected to thermohygro-metric cycles stress as rising damp effects. The specific geometry of the composite specimens has allowed to test the adherence between dehumidified repair plaster and masonry structures, in order to prequalify the durability of the repair product. The notch tips have put to the test the adherence of the repair plaster applied to the stone support, simulating the fatigue loads that can compromise the restoration work.

The Teflon sheet, inserted at the contact surface between the upper and lower wedge, was able to reduce the friction and to stabilize the load curves. The static compressive tests represent a rather fast laboratory procedure useful for analyze the delamination of the dehumidified repair plasters applied to the historical masonry of the Sacro Monti di Varallo. The next step of this experimental research, at the moment in progress, is to carry out the cyclic compressive tests in order to simulate the fatigue stress between the masonry stone and the repair mortar.

The experimental tests can be carried out by several and different dehumidified mortars in order to compare their mechanical behavior.

4. Conclusions

Experimental procedures have been described to validate the choice of a durable repair mortar against different stress stresses (including thermal stresses) and compatible with the mechanical characteristics of the historical masonry. The experimental methodology is useful to identify a number of key parameters for interpreting the long-term behavior of historic brick-strengthening mortar system. The results showed a considerable change of mechanical characteristics in strengthening materials due to maturation, thermo-hygrometric and various fatigue loading condition that can affect masonry structure after restoration process, according to the experimental results of previous researches [3, 5]. In this way it is possible avoid errors associated with materials that are not mechanically compatible. The experimental procedure described above studied in depth previous researches on the creep of single materials [6–8] and historical walls [4, 5, 9, 10], shifting the focus on the analysis of the long-term behavior of the new strengthening materials applied to historical masonry structures. The tests have allowed to select the most compatible and durable restoration product and technique for strengthening work in the Royal Palace of Venaria Reale.

In parallel an innovative laboratory procedure for pre-qualification of dehumidified repair mortars applied to historical masonry buildings has been described. The specific geometry of mixed stone-mortar specimens can test the de-bonding process of mortar in adherence with the historical masonry structures. This method supplies useful indication to select, from a range of alternatives, the repair product that is best in keeping with the mechanical characteristics of historical material. The experimental procedure is currently being used at Sacro Monte di Varallo Special Natural Reserve, where the historical stone masonry of the Chapels are subjected to rising damp effects due to capillary action or rain infiltrations. The study of the phenomena involved in the de-bonding process between the masonries stone and the dehumidified repair plasters is basic to plan a durable restoration work of the historical plasters of the Chapels.

Author details

Alessandro Grazzini

Address all correspondence to: alessandro.grazzini@polito.it

Politecnico di Torino, Turin, Italy

References

- [1] Valluzzi MR, Binda L, Modena C. Experimental and analytical studies for the choice of repair techniques applied to historic buildings. *Materials and Structures*. 2002;35: 285-292. DOI: 10.1007/BF02482134

- [2] Bocca P, Grazzini A. Mechanical properties and freeze-thaw durability of strengthening mortars. *Journal of Materials in Civil Engineering*. 2013;**25**:274-280. DOI: 10.1061/(ASCE)MT.1943-5533.0000597
- [3] Mutluturk M, Altindag R, Turk G. A decay function model for the integrity loss of rock when subjected to recurrent cycles of freezing-thawing and heating-cooling. *International Journal of Rock Mechanics and Mining Sciences*. 2004;**41**:237-244. DOI: 10.1016/S1365-1609(03)00095-9
- [4] Anzani A, Garavaglia E, Binda L. Time dependent behaviour of historic masonry: A probabilistic model. In: *Proceedings of the 7th International Masonry Conference; October 30–November 1, 2006; London*. British Masonry Society [CD-ROM]
- [5] Anzani A, Binda L, Mirabella Roberti G. The effect of heavy persistent actions into the behaviour of ancient masonry. *Materials and Structures*. 2000;**33**:251-261
- [6] Minh-Tan D, Chaallal O, Aitcin PC. Fatigue behaviour of high-performance concrete. *Journal of Materials in Civil Engineering*. 1993;**5**:96-111
- [7] Mu B, Shah SP. Fatigue behavior of concrete subjected to biaxial loading in the compression region. *Materials and Structures*. 2005;**38**:289-298. DOI: 10.1617/14155
- [8] Taliercio A, Gobbi E. Experimental investigation on the triaxial fatigue behaviour of plain concrete. *Magazine of Concrete Research*. 1996;**48**:157-172. DOI: 10.1680/mac.1996.48.176.157
- [9] Carpinteri A, Grazzini A, Lacidogna G, Manuello Bertetto A. Durability evaluation of reinforced masonry by fatigue tests and acoustic emission technique. *Structural Control and Health Monitoring*. 2014;**21**:950-961. DOI: 10.1002/stc.1623
- [10] Bocca P, Lacidogna G, Grazzini A, Manuello Bertetto A, Masera D, Carpinteri A. Creep behaviour in reinforced masonry walls interpreted by acoustic emission. *Key Engineering Materials*. 2010;**417-418**:237-240. DOI: 10.4028/www.scientific.net/KEM.417-418.237
- [11] Brooks JJ, Abu Bakar BH. Shrinkage and creep of masonry mortar. *Materials and Structures*. 2004;**37**:177-183. DOI: 10.1007/BF02481617
- [12] Fassina V, Favaro M, Naccari A, Pigo M. Evaluation of compatibility and durability of a hydraulic lime-based plaster applied on brick wall masonry of historical buildings affected by rising damp phenomena. *Journal of Cultural Heritage*. 2002;**3**:45-56. DOI: 10.1016/S1296-2074(02)01158-5
- [13] Barpi F, Valente S. Lifetime evaluation of concrete structures under sustained post-peak loading. *Engineering Fracture Mechanics*. 2005;**72**:2427-2443. DOI: 10.1016/j.engfracmech.2005.03.010
- [14] Barpi F, Valente S. The cohesive frictional crack model applied to the analysis of the dam-foundation joint. *Engineering Fracture Mechanics*. 2010;**77**:2182-2191. DOI: 10.1016/j.engfracmech.2010.02.030
- [15] Bocca P, Grazzini A, Masera D, Alberto A, Valente S. Mechanical interaction between historical brick and repair mortar: Experimental and numerical tests. *Journal of Physics: Conference Series*. 2011;**305**:1-10. DOI: 10.1088/1742-6596/305/1/012126